Seam Defects in Bar Rolling with Consideration of Billet Geometries and Surface Scale Conditions

WEI-YI CHIEN and YI-LIANG OU

Iron & Steel Research & Development Department,
China Steel Corporation

In this paper, the influence of billet geometries and surface scale conditions on seam defects in the bar rolling process is investigated. With the assumption that seam defects might be formed by the material buckling on the billet surface, the generation of seam defects in the bar rolling process is investigated by a three-dimensional elastic-plastic finite element analysis that accounts for the corner radius and surface scale conditions of the billet. Experimental validations with different corner radii of billets are also carried out in the bar mill. The geometric effect of billets with surface scale on the formation of seam defects based on the finite element analysis is in agreement with that based on the experiments. The results indicate that the seam defects can be reduced by increasing the corner radius or decreasing the thickness of surface scale on billets.

Key words: Surface Defects, Bar Rolling, Finite Element Analysis

1. INTRODUCTION

Seams are the most common defects encountered in the bar rolling process. Since seam defects are harmful during the secondary cold forging process, bar products with seam defects must be rejected as scrap which is very costly for the production line. As the present market demands for high quality bar products increase, it is of great importance to minimize such defect formations on the surface of rolled bars.

Seam defects are small cracks on the surface of bar products. Figure 1 shows a close-up view of the seam defect observed after the bar rolling process. In general, the depths of seam defects are in the range of 0.01~ 0.05mm. It is not easy to detect such a defect because it is hidden under the skin of the bar surface. Therefore, upsetting tests are often conducted with cylindrical specimens to reveal the existence of seam defects as shown in Fig.2.

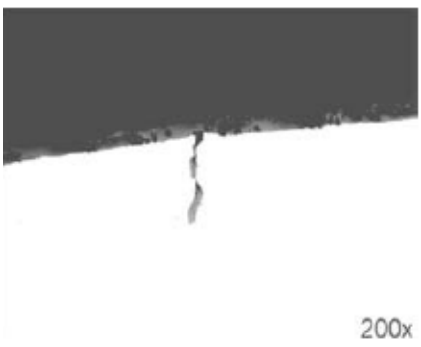

Fig.1. A close-up view of the seam defect

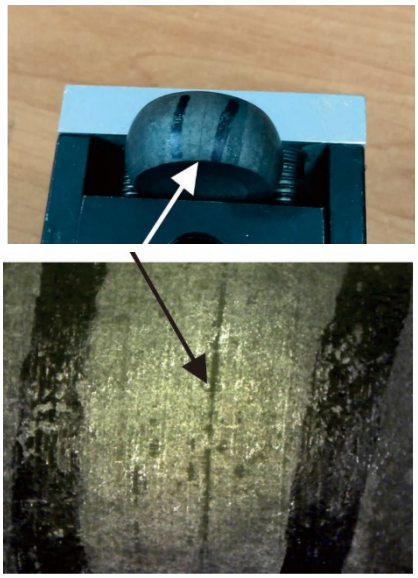

Fig.2. The upsetting test of a cylindrical specimen.

There are many sources for seam defect formation. Seam defects can originate from steel making, casting, or during the rolling process. In order to improve the surface quality of the final products, it is common to grind the billet surfaces before rolling in order to remove the

defects from continuous casting. However, seam defects can be found from the improper mill practices such as improper roll pass design, damaged roll surfaces, worn out grooves and coarse scales rolled into the surface of the rolled product.

In the bar rolling process, the deformation behavior of the rolled billets is very complex. In order to establish methods to predict surface defects as a function of rolling conditions, Kushida et al.[1] rolled a lead alloy with copper plating and a lead alloy without plating in a laboratory mill. The deformed shapes of test samples were compared after rolling. The results indicated that the surface defects are caused by plastic buckling and can be promoted by hardening the surface. In CSC, it is found that the seam defects are highly correlated with the existence of the surface scale, which is significantly harder than the base metal. For example, for the chromium-molybdenum steel such as SCM435, it is difficult to remove the surface scale of the billet by using normal pressurized water. Consequently, seam defects are common for such material. This interpretation can be further validated from the fact that the scales in the seam defects contain chromium in SCM435 from SEM analysis.

In this paper, the influence of billet geometries and surface scale conditions on the generation of seam defects in the bar rolling process is investigated numerically and experimentally. The finite element analysis is first employed to model the variations of corner radii and the surface scale conditions of billets. Experimental validations with different corner radii of billets are then carried out in the bar mill. Finally, the geometric effects of the billet with the surface scale on the formation of seam defects are compared based on the finite element analysis and experiments, respectively.

2. FINITE ELEMENT MODEL

The finite element analysis was carried out to simulate the bar rolling with three different billet geometries (R0: square billet, R14: corner radius=14mm, and R20: corner radius=20mm) to investigate the deformation behavior of the billet during the first roughing pass. Because of the symmetry of the billet and the rolling boundary conditions, only one quarter of the billet is modelled. An example of the finite element model used for computation is shown in Fig.3. The billet material is modelled as elastic-plastic isotropic hardening material and von Mises yield criterion is used. The roll is considered as a rigid body with constant angular velocity. The billet material is modelled by eight node isoperimetric brick elements with reduced integration. In this paper, the chromium-molybdenum steel SCM435 is considered in the analysis. In order to obtain the stress-strain curves of SCM435 at high temperature, the hot compression tests were carried out using Gleeble under the strain rate of 1 at CSC's research laboratory. The stress-strain relations with temperature varying from 900°C to 1150°C are shown in Figure 4 and employed in the finite element analysis.

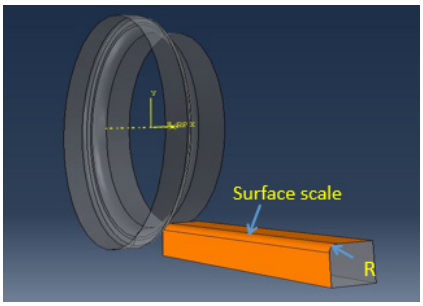

Fig.3. An example of the finite element model.

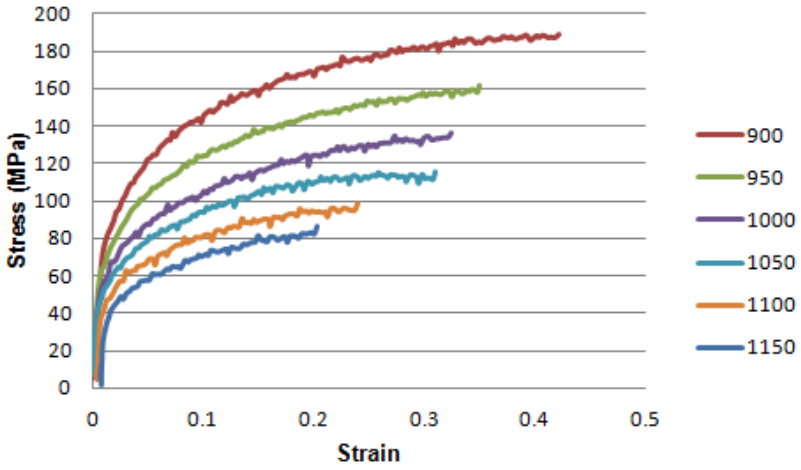

Fig.4. The stress-strain curves of SCM435 at various temperatures.

Since the existence of surface scale can affect the deformation behavior of the billet in the rolling process, the billets with surface scale and without surface scale are both considered in the analysis, respectively. The scale is modeled using shell elements attached to the billet surface. Based on the previous research works[2, 3], the strength of the scale is multiplied by a factor of 5 with respect to that of the base material.

3. SIMULATION RESULTS

Figure 5 shows the angular distributions of equilibrium plastic strain along the billet surface without the scale for three different billet geometries. The results are expressed in terms of the cylindrical coordinates with respect to the center of the billet as shown in the figure. Note that 0° represents the vertical upward direction as shown in Fig.5. As shown in the figure, the maximum equilibrium plastic strain for the square billet (R0 case) is near 1 around $\theta = 58^\circ$ whereas the maximum equilibrium plastic strains for the other two cases (R14 and R20) are significantly lower. The equilibrium plastic strain decreases as the corner radius increases (R0>R14> R20). Here, attention must be paid not only the magnitude of the equilibrium plastic strain, but also the gradient of the equilibrium plastic strain around the billet corner. When the corner radius is increased to 20mm, the distribution of the equilibrium plastic strain is smooth around the billet corner, and no obvious peak value is observed.

Figure 6 shows the angular distribution of equilibrium plastic strain along the billet surface with the scale for three different billet geometries. The thickness of the scale is assumed to be 0.3mm. Similarly, the maximum equilibrium plastic strain is near the billet corner. The equilibrium plastic strain also decreases with increasing the corner radius. It should be noted that even for the

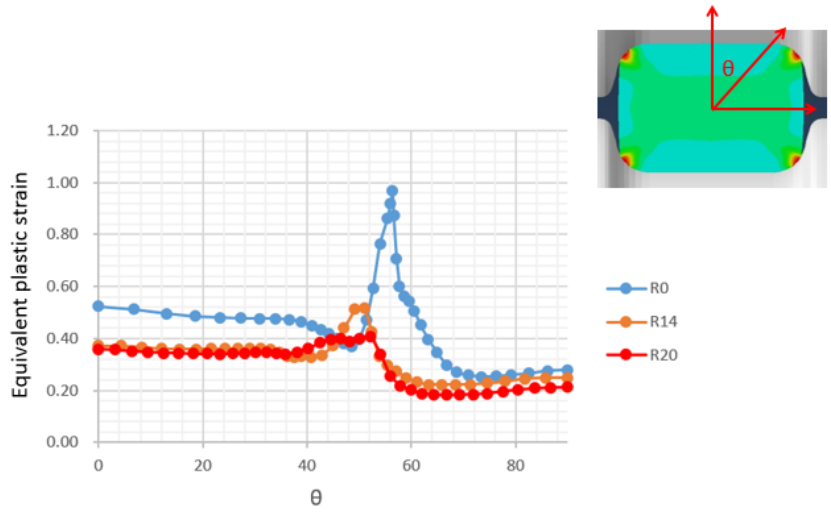

Fig.5. The angular distributions of equilibrium plastic strain along the billet surface without scale

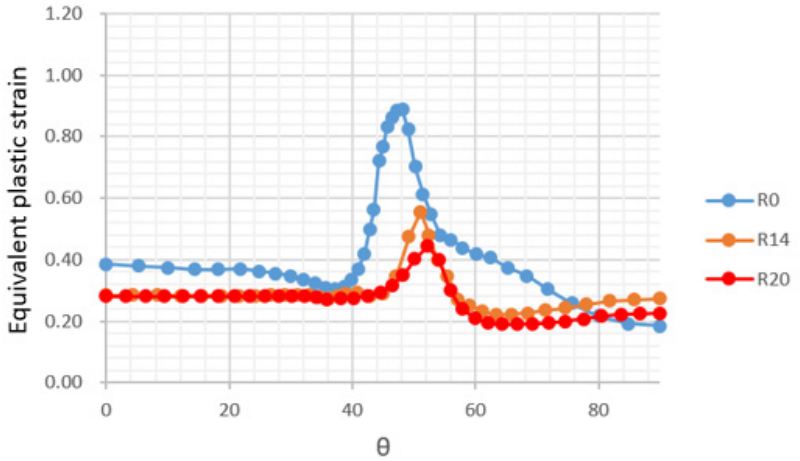

Fig.6. The angular distributions of equilibrium plastic strain along the billet surface with scales

corner radius equals 20mm, the peak value of the equilibrium plastic strain is still obvious. Therefore, the existence of the surface scale induces the discontinuity of the plastic strain in the local area of the billet corner.

In order to capture the material buckling characteristics in the rolling process, Fig.7 shows the billet contours before and after rolling for different corner radii and surface scale conditions. Figure 8 is a 3D representation for the cases in Fig.7. In Fig.8, only the characteristic lines, defined as the angle between the normal vectors of two adjacent elements greater than 20°, are shown. In Fig.7 and 8, it is shown that the wrinkles occur on the billet surface where the material buckling behavior is promoted as the corner radius decreases and the

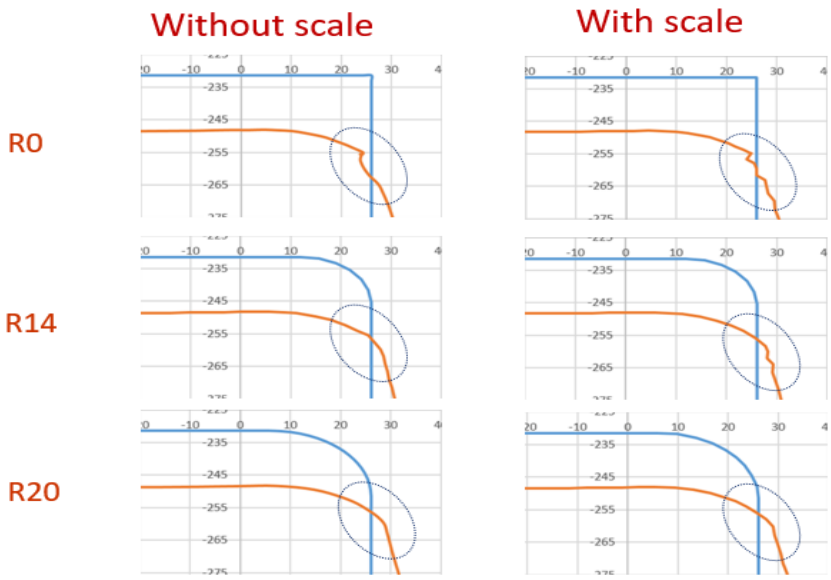

Fig.7. The billet contours before and after rolling for different corner radii and surface scale conditions (blue: before rolling, brown: after rolling).

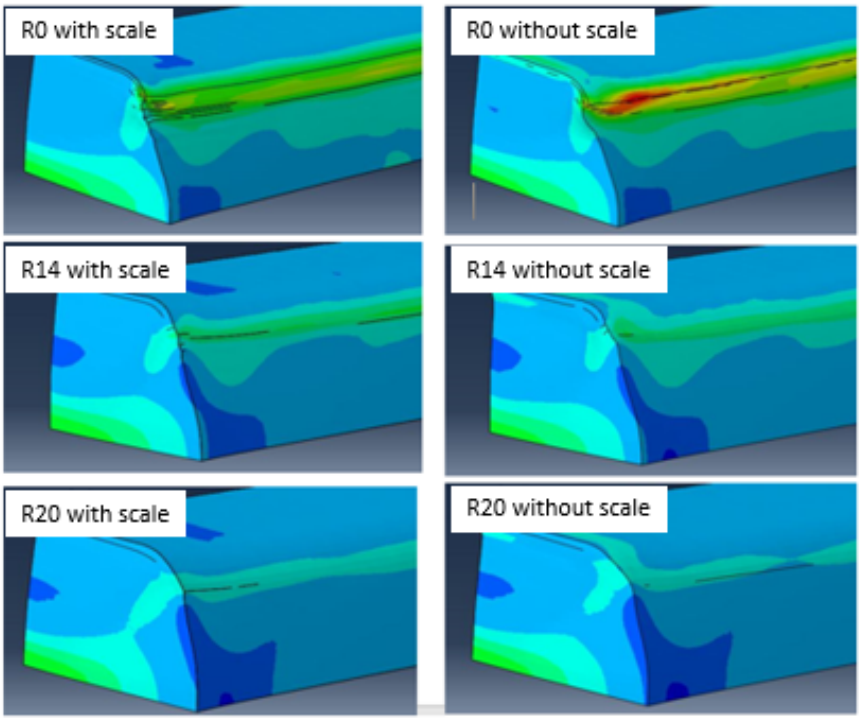

Fig.8. A 3D representation for the cases in Figure 7

surface scale exists. For the corner radius equals 14mm, which is used in CSC, the seam defects due to the material buckling might appear with the existence of the surface scale. However, if no surface scale exists, the material buckling disappears. This is consistent with the fact that few seam defects are found if the surface scale is removed effectively in the rolling process. If the corner radius increases to 20mm, no significant material buckling was observed no matter if the surface scale exists or not.

Depending on heating time, temperature, and the condition of the descaling facility, the thickness of the surface scale is different. Figure 9 shows the billet contours before and after rolling based on the current CSC billet geometry for three different thicknesses of the surface scale (0.05mm, 0.3mm, and 1mm). In the figure, it can be seen that as the thickness of the surface scale increases, the level of the material buckling becomes severe. Therefore, if the descaling efficiency can be enhanced, the seam defects may be reduced even without totally avoiding the existence of the surface scale.

4. EXPERIMENTAL VALIDATION

In order to validate the results of the finite element analysis, four SCM 435 experimental billets with two different corner radius are prepared. The experimental billets are rolled in sequential order such that the rolling conditions can be considered identical. After the rolling process, upsetting tests are carried out using specimens machined from the experimental rolled products. The results are summarized in Table 1. In the 5th loop, the average defective rates in upsetting tests are similar for both cases. However, the defects might be due to the scratch resulting from the contact with roll guides since the rolling process is more unstable in the head part of the billets. In the 10th and the 15th loops, the average

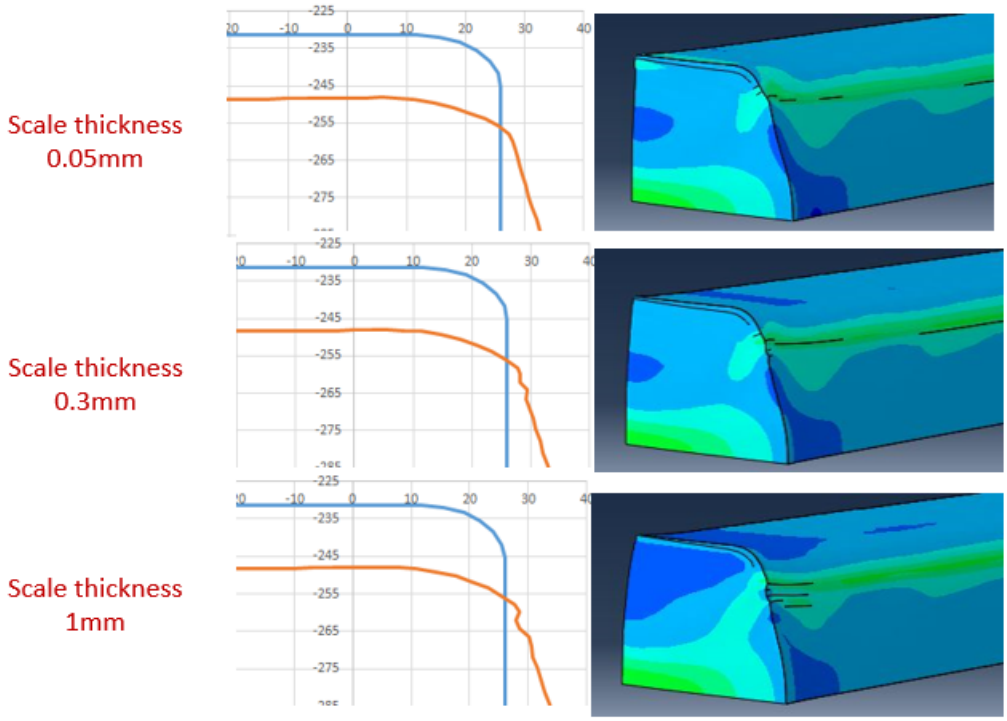

Fig.9. The billet contours before and after rolling for different thicknesses of the surface scale (blue: before rolling, brown: after rolling).

Table 1 Average defective rate in upsetting tests

Corner type	Average defective rate in upsetting tests		
	5th loop	10th loop	15th loop
Small radius	5.0%	2.8%	0.8%
Large radius	5.2%	1.8%	0%

defective rates in upsetting tests in large radius cases are smaller than those in the small radius one. The results show that the defects can be reduced with the increasing corner radius.

5. CONCLUSIONS

The influence of billet geometries and surface scale conditions on seam defects in the bar rolling process is investigated by finite element analysis. The billets with different corner radii and surface scale conditions are modeled in the bar rolling process. The surface scale is considered as a hard surface layer on the billet. The simulation results indicate that the surface scale of the billet can promote the occurrence of seam defects. However, the formation of seam defects can be reduced with increasing the corner radius of the billet. The experimental validation is carried out in the bar mill by rolling the billets with different corner radii. The results are in agreement with those based on the finite element analysis.

REFERENCES

1. H. Kushida, Y. Maeda, H. Kakimoto, T. Ishikawa, and S. Sugyo, Surface Defect Generation Behavior of Wire Rolling - Analytical Study of Rolling Conditions and Experimental Verifcation of Surface-Hardened Layer, Tetsu-to-Hagane, 2014, vol. 100, pp. 1535-1541.
2. M. Takeda, T. Onishi, S. Nakakubo, and S. Fujimoto, Physical Properties of Iron-Oxide scales on Si-containing Steels at High Temperature, Materials Transaction, 2009, vol. 50, pp. 2242-2246.
3. M. Nanko, 鉄鋼材料に生成する酸化スケールの機械的特性, Form Tech Review, 2010, vol. 19, pp. 52-55. □